

Dust Evolution from Nearby Galaxies: Bridging the Gap Between Local Universe and Primordial Systems

Frédéric Galliano¹

¹Department of Astronomy, University of Maryland, College Park, MD 20742, USA
email: galliano@astro.umd.edu

Abstract. This paper presents the results of a study aimed at understanding the evolution of the dust properties, as a function of both the environmental conditions and the metal enrichment of the system. I first review the peculiar dust properties of dwarf galaxies, and discuss attempts to understand their origin. Then, I discuss the evolution of the PAH and dust abundances, constrained by the UV-to-radio SED of nearby galaxies, comparing the properties of low-metallicity environments and more evolved systems. I discuss the long term evolution of dust in galaxies, comparing the grain production by various stellar progenitors to their destruction by SN blast waves and in H II regions. Finally, I will show how these models explain the paucity of PAHs in low-metallicity environments.

Keywords. stars: AGB, supernovae: general, ISM: abundances, ISM: dust, ISM: extinction, galaxies: dwarf, galaxies: evolution, galaxies: high-redshift, galaxies: starburst, infrared: galaxies

1. Introduction

Understanding the variations of dust properties with the age and physical conditions of a system has become crucial for comprehending galaxy evolution. Indeed, the wide database of infrared observations collected by the *Infrared Space Observatory* and the *Spitzer Space Telescope*, with an unprecedented quality, provides valuable observational constraints of the elementary evolutionary processes playing a role in the interstellar medium (ISM). How do dust abundances vary with metallicity? What processes affect the composition and size distribution of dust grains? How is the dust distributed throughout the various phases of the ISM? Answers to these fundamental questions are necessary to address the following higher level outstanding issues. How is the infrared spectral energy distribution (SED) of a whole star forming galaxy related to its physical conditions and star formation history? What were the ISM properties of the first galaxies formed?

These questions can be addressed from different points of view. The local approach consists in observing an individual region or object (SN II, AGB star, shock, PDR, etc.), in order to derive detailed information on a few particular processes. The difficulty of this approach is that such regions, accessible to current observatories, are not very numerous. On the opposite, the global approach – that I am going to discuss in this paper – consists in observing an entire galaxy, in order to derive average properties. The observations are easier in this case, although the difficulty of this approach is that all the individual processes are mixed, and not easily separable.

Nearby dwarf galaxies constitute extremely useful laboratories to address these questions, since they can be considered as snapshots of galaxy evolution at early epochs of their aging, due to their low elemental enrichment. In that sense, dwarf galaxies are

also important objects to understand protogalaxies. Although dwarf galaxies are not rigorously identical to primordial systems, their study provides insights on the interplay between star formation and the ISM in low-metallicity environments. Moreover, the ISM of dwarf galaxies experiencing massive star formation is subjected to extreme conditions of radiation and numerous supernovae (SN) blast waves, providing unique constraints on the impact of these processes on the ISM.

This paper summarizes an original study aimed at understanding the origin of the weakness of the mid-IR bands in low-metallicity environments.

2. The Peculiar Infrared Properties of Low-Metallicity Environments

To begin with, dwarf galaxies do not constitute an homogeneous population of objects – they are a category by default. This category roughly encompasses systems with metal abundances lower than solar ($12 + \log(\text{O}/\text{H})_{\odot} \simeq 8.8$), as a consequence of the size-metallicity relation (e.g. Kunth & Östlin 2000). Therefore, it is very difficult to characterize them by an ensemble of well-defined properties. Alternatively, we are compelled to describe how their properties differ from normal metallicity systems and to derive trends between these properties.

The first infrared SEDs of dwarf galaxies were provided by *IRAS* (Hunter *et al.* 1989), and showed what optical studies suggested: a lower dust-to-gas mass ratio compared to the Galaxy. It was not until the times of the *Infrared Space Observatory* that the mid-IR properties and their spatial distribution could be studied in details. It appeared that starbursting dwarf galaxies presented similarities with giant Galactic H II regions: lack of polycyclic aromatic hydrocarbons (PAH) and steep rising mid-IR continuum (Thuan *et al.* 1999; Madden *et al.* 2006). Self-consistent modeling of the UV-to-mm SED of nearby blue compact galaxies by Galliano *et al.* (2003, 2005) confirmed these views and showed that the difference in observed properties could be explained by a systematic difference in intrinsic grain properties. In this model, the dust grains are eroded and fragmented by the numerous SN shock waves sweeping the ISM, accounting for the peculiar shape of their Magellanic-like extinction curves and their IR SED. In addition, this study reported the presence of a submillimetre emission excess which can be attributed to very cold, shielded dust ($T \lesssim 10$ K). The significant amount of dust potentially hidden in these dense clumps, challenges our comprehension of dust evolution and ISM structure.

The exceptional sensitivity of *Spitzer* brought to this field tremendous advances. The spatial variations of the IR properties of several low-metallicity systems (like NGC 6822 Cannon *et al.* 2006) as well as the Magellanic clouds (Meixner *et al.* 2006; Bolatto *et al.* 2007) have been studied. *Spitzer* also allowed better statistics by reaching fainter sources (Engelbracht *et al.* 2005; Wu *et al.* 2006). In particular, it became clear that there was a trend between the strength of the aromatic features and the metallicity.

The believed carriers of these aromatic features, the PAHs, are known to be destroyed in H II regions by the hard UV radiation (e.g. Cesarsky *et al.* 1996). Madden *et al.* (2006) proposed that, due to the lower opacity of the ISM in dwarf galaxies – which is a consequence of the lower metal abundance – the hard UV photons penetrate deeply and destroy the PAHs on larger scale, than in normal metallicity systems. This interpretation is based on the correlation of left panel of Fig. 1. On the other hand, O'Halloran *et al.* (2006) proposed that the PAHs could be widely destroyed by the numerous shock waves that sweep these galaxies (right panel of Fig. 1). However, observations of individual supernovae indicate that not only the PAHs, but also the carriers of the underlying continuum are destroyed by the shock (e.g. Reach *et al.* 2002).

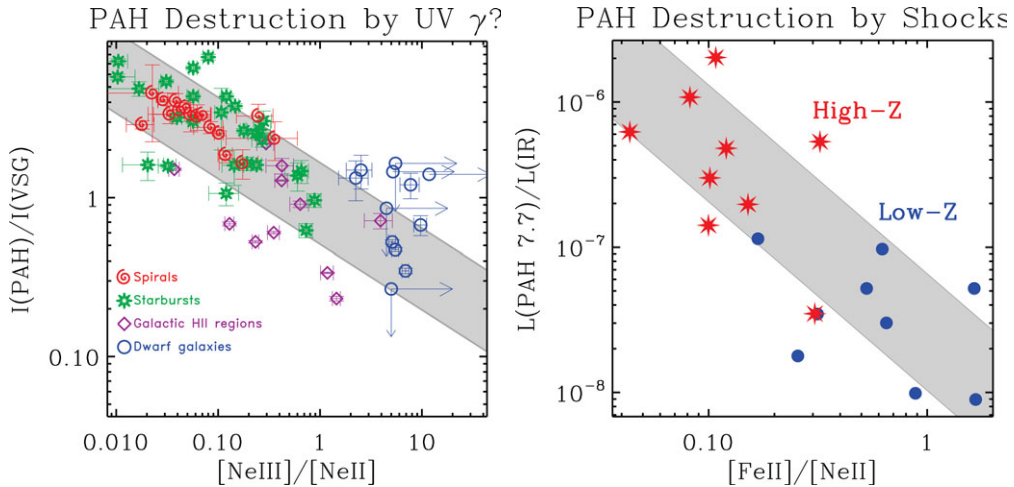


Figure 1. Two explanations for the paucity of PAHs in low-metallicity environments. **Left:** correlation of the PAH strength with the $[\text{NeIII}]_{15.56\mu\text{m}}/[\text{NeII}]_{12.81\mu\text{m}}$ ratio (Madden *et al.* 2006). The PAH intensity is normalised to the intensity of the very small grain (VSG) continuum. The $[\text{NeIII}]/[\text{NeII}]$ ratio is very sensitive to hard UV photons, and provides therefore a tracer of ionizing stellar populations. **Right:** correlation of the PAH strength with the $[\text{FeII}]_{25.99\mu\text{m}}/[\text{NeII}]_{12.81\mu\text{m}}$ ratio (O’Halloran *et al.* 2006). The iron being mostly depleted into dust, its observation in the gas phase is presumed by the authors to be an indication of its sputtering by SN II shock blasts. Thus, O’Halloran *et al.* (2006) consider the $[\text{FeII}]/[\text{NeII}]$ ratio to be a shock tracer.

These explanations are based on observed feature intensities, which depend both on the PAH abundance and on their irradiation. To understand the origin of these relations and interpret them correctly, the derivation of the actual PAH abundance is needed.

3. Global SED Modeling of Nearby Galaxies

Derivation of the PAH abundances in galaxies from their observed mid-IR spectral features is complicated by the nature of their emission mechanism. PAHs are stochastically-heated by the interstellar radiation field (ISRF) and consequently only a fraction of their population is copiously emitting IR radiation at any given time. Correcting for the mass of PAHs too cold to radiate at mid-IR wavelengths requires detailed modeling of their stochastic heating process, and therefore detailed knowledge of the ISRF. The situation is further complicated by the fact that a significant fraction of the mid-IR emission originates from hot dust in H II regions radiating at the equilibrium dust temperature. Deriving the abundance of PAHs and other dust species in a galaxy requires therefore careful modeling of the stellar population that produces the ISRF that heats the dust in the diffuse ISM and the ionizing radiation that heats the dust in H II regions.

We constructed a self-consistent model for the evolution of the stellar populations and the composition of the ISM in a sample of 35 nearby galaxies, with metallicities ranging from $1/50$ to $\simeq 2 Z_{\odot}$. The star formation history comprises of two distinct components: (1) a global continuous mode of star formation which is used to calculate the chemical evolution with a closed-box model, and the evolution of the stellar radiation using the PÉGASE stellar population code (Fioc & Rocca-Volmerange 1997); and (2) an “instantaneous burst” of star formation (age $\lesssim 10$ Myr). This short-lived burst does not contribute significantly to the metallicity of the gas, and is tailored to fit the observed UV, optical, radio, and the IR emission from dust in H II regions. The continuous star formation

component provides a self-consistent picture of the evolution of stellar colors and metallicity as a function of age in all the galaxies in the sample. The relative contribution of these two components, as well as the age of the galaxy are fully constrained by the UV-to-radio continuum emission. Details of the models are presented in Galliano *et al.* (2008a).

The following describes the steps used to decompose the observed galactic SEDs into the various stellar and ISM emission components (see Fig. 2).

(a) We first decompose the radio continuum into free-free and synchrotron emission in order to constrain the emission measure from the galaxy.

(b) The resulting free-free continuum, together with observations of the mid-IR continuum between $\simeq 5$ and $\simeq 60 \mu\text{m}$ are used to constrain the gas density and reradiated energy from the H II regions. We assume that any existing PAHs are destroyed inside the H II regions, and use a simple radiative transfer model (Galliano *et al.* 2008a) to calculate the absorbed radiation that is emitted as free-free emission from the gas, and thermal IR emission from the dust in the H II region.

(c) Optical and near-IR broadband emission are used to constrain the radiation escaping from the H II regions and that from the non-ionizing stars. They comprise the ISRF that heats the dust in PDRs.

(d) The observed far-IR/submm SED constrains the dust emission from the PDRs. The PAH-to-dust mass fraction is constrained by the detailed fit of the features seen on the mid-IR spectrum.

(e) Globally, the stellar luminosity absorbed by the gas and dust phases of the ISM is equal to the total reradiated and escaping power from the galaxy.

4. Dust Evolution in Galaxies

The model described in Sect. 3, when applied to the observations of each galaxy in our sample, provides the variation of PAH and dust abundances in galaxies, as a function of metallicity. Similar trends of dust abundances with metallicity have also been presented by Draine *et al.* (2007) and Engelbracht *et al.* (2008). However, Draine *et al.* (2007) used a much simpler SED without constraints from the mid-IR spectroscopy. Engelbracht *et al.* (2008) did not estimate the PAH masses. None of them provide a consistent interpretation of these trends.

To interpret these trends, we have developed the following dust evolution model (Galliano *et al.* 2008a, Fig. 3).

(a) We consider a closed box model. The star formation rate (SFR) follows the Kennicutt (1998) law, relating the surface densities of the gas to the surface density of the SFR. We adopt a Salpeter IMF.

(b) At any time, we follow the evolution of stars of different masses, until they release their elements into the ISM. Massive stars, evolving into supernovae have a short lifetime of a few Myr and therefore inject their elements promptly, while low-mass stars evolve to their post-AGB phase after $\simeq 400$ Myr.

(c) For each stellar progenitor, the elements are combined to form various types of grains (carbon, silicates, titanium oxydes, etc.).

(d) A fraction of the elements locked-up in the grains is returned to the gas phase, when sputtered by a shock wave. We parametrize the dust destruction efficiency by SN II blast waves by considering that all the dust is destroyed around a supernovae, within a volume determined by the mass of gas (m_{ISM}) it encloses. Therefore, the dust destruction is proportional to the supernova rate. We vary $\langle m_{\text{ISM}} \rangle$ between $0 M_{\odot}$ (no destruction)

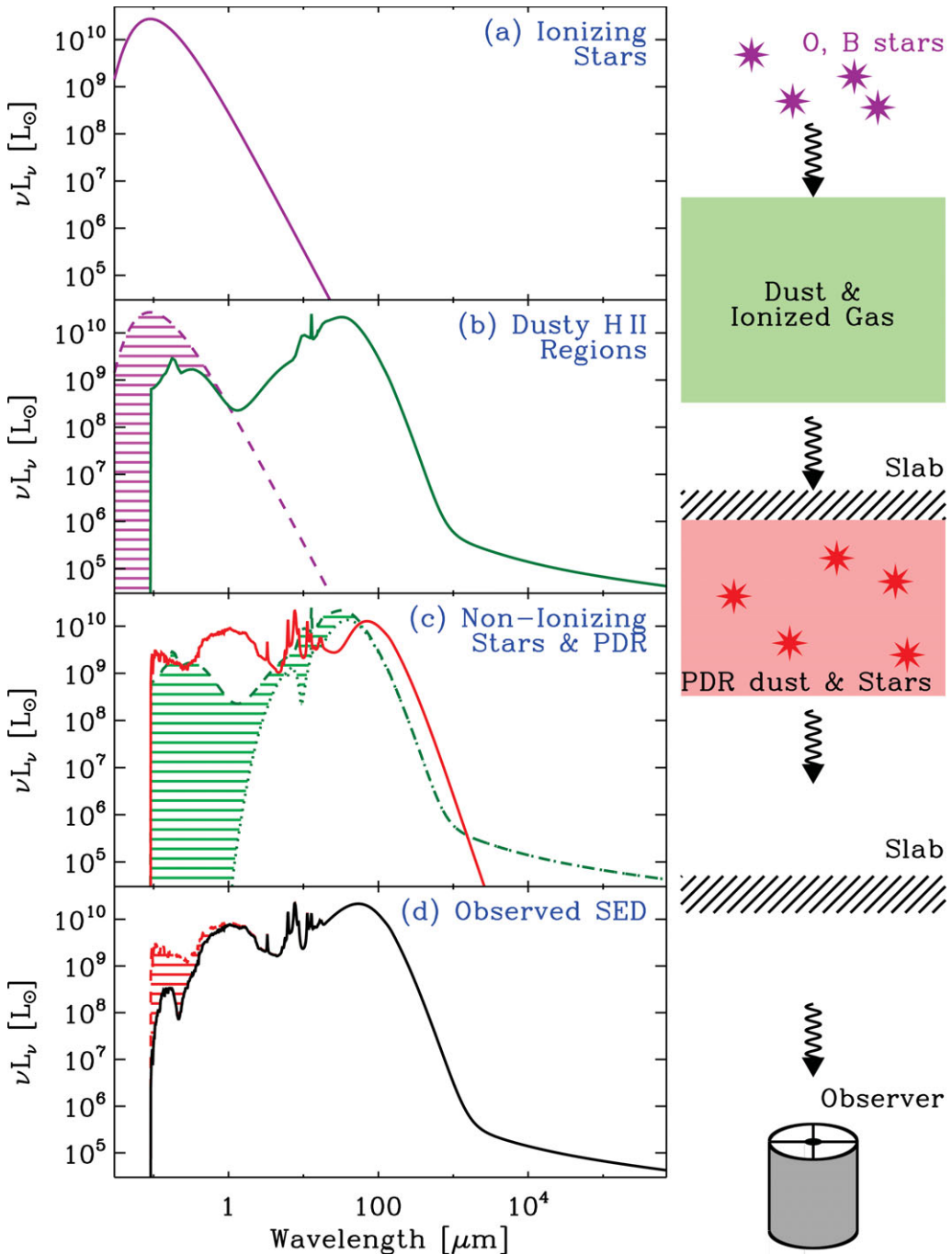


Figure 2. Schematic illustration of the of the model used to decompose the observed galactic SED into the various stellar and ISM emission components (Galliano *et al.* 2008a). **Panel (a):** SED of the ionizing stars (purple curve). **Panel (b):** IR spectrum of the dust in the H II regions (green curve). **Panel (c):** Stellar emission and emission from dust residing in the neutral ISM (red curve). **Panel (d):** The observed SED after passing through a slab of internal extinction (black curve). In each figure, the hatched region represents the emission from the previous panel that is absorbed by the relevant phase depicted in the panel.

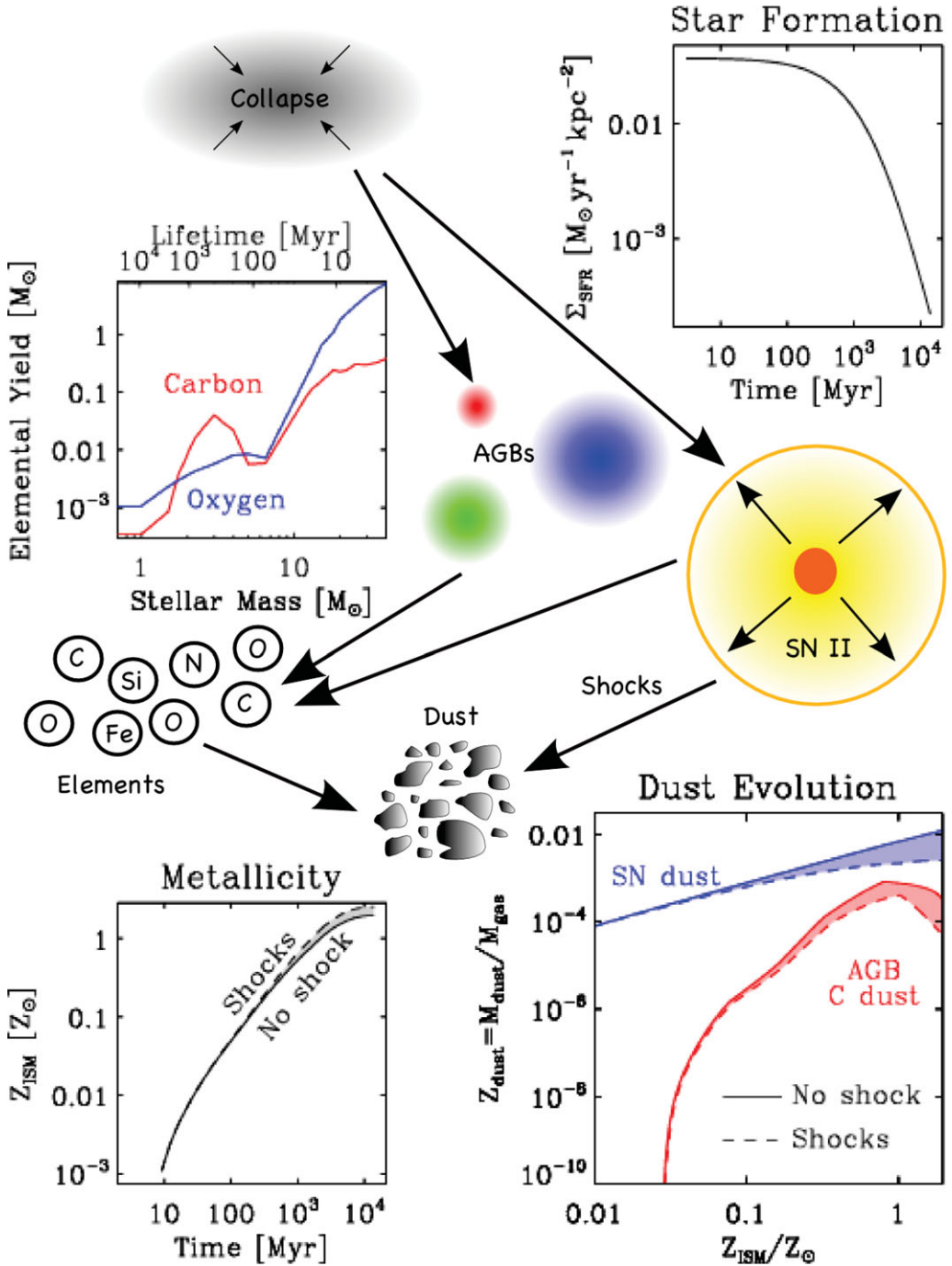


Figure 3. Flow chart of the dust evolution model. (1) We start from the collapse of a cloud, following the star formation rate given in the top right panel. (2) Stars of different masses and lifetimes are produced at any time. When these stars die, they release their elements in the ISM (top left panel). (3) These elements contribute to the metallicity of the gas (bottom left panel). A fraction of the elements are combined to form different kinds of dust species (bottom right panel). (4) Some of these grains are destroyed by the SN II blast waves.

and $300 M_{\odot}$ (Galactic value). The two bottom plots of Fig. 3 demonstrate the effects of this parameter.

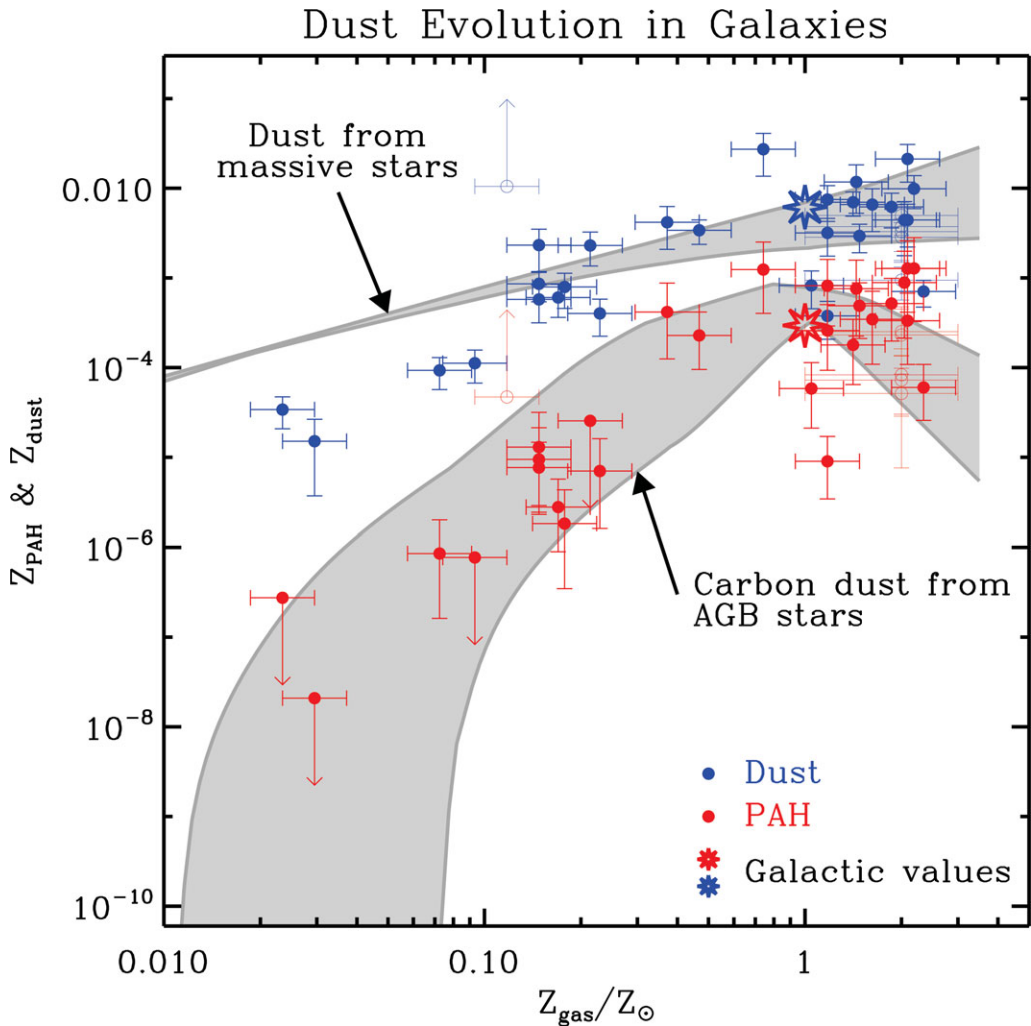


Figure 4. Comparison between observed and theoretical trends of PAH and dust abundances with metallicity (Galliano *et al.* 2008a). Z_{PAH} and Z_{dust} are respectively the PAH- and dust-to-gas mass ratios and Z_{gas} is the metallicity of the gas. The error bars are the results of the SED modeling. The grey filled curves are the results from the dust evolution model.

Fig. 4 shows the comparison between the observed trends of PAH and dust abundances with metallicity and the theoretical dust evolution in galaxies.

First, the observed PAH trend is in good agreement with the trend of carbon dust produced in AGB stars. Indeed, AGB stars are believed to be the principal source of PAHs. This trend provides a natural explanation of the paucity of PAHs in low-metallicity environments: due to their long lifetime ($\simeq 400$ Myr), AGB stars begin to contribute to the injection of PAHs in the ISM, when the galaxy is already evolved. Therefore, there is a delay between the dust and the PAH contributions, and this delay translates into metallicity.

Second, the trend of the other dust components is in good agreement with the production of grains by SN II, down to $\simeq 1/10 Z_{\odot}$. At very low-metallicities, the observed dust-to-gas mass ratios are systematically lower than the SN II dust. A significant mass of cold dust could have been overlooked because these galaxies lack submillimeter data. Another possible origin of this disagreement could be that the star formation history of these galaxies is not continuous as in our dust evolution model.

The SN II yield (mass of dust formed by an average SN II) of this model is relatively high (consistent with the $\simeq 1 M_{\odot} \text{SN}^{-1}$ derived from observations of distant quasars; Dwek *et al.* 2007), compared to estimates on individual SN II ($\simeq 0.05 M_{\odot} \text{SN}^{-1}$; Rho *et al.* 2008). This discrepancy between the global and the local approaches is one the main challenge in dust evolution, nowadays. The *Herschel* satellite, by extensively observing submillimeter wavelengths, will provide important constraints on the dust masses, and help address this issue.

References

- Bolatto, A. D., Simon, J. D., Stanimirović, S., *et al.*, 2007, *ApJ*, 655, 212
Cannon, J. M., Walter, F., Armus, L., *et al.*, 2006, *ApJ*, 652, 1170
Cesarsky, D., Lequeux, J., Abergel, A., *et al.*, 1996, *A&A*, 315, L305
Draine, B. T., Dale, D. A., Bendo, G., *et al.*, 2007, *ApJ*, 663, 866
Dwek, E., Galliano, F., & Jones, A. P. 2007, *ApJ*, 662, 927
Engelbracht, C. W., Gordon, K. D., Rieke, G. H., *et al.*, 2005, *ApJL*, 628, L29
Engelbracht, C. W., Rieke, G. H., Gordon, K. D., *et al.*, 2008, *ApJ*, 678, 804
Fioc, M. & Rocca-Volmerange, B. 1997, *A&A*, 326, 950
Galliano, F., Dwek, E., & Chantal, P. 2008a, *ApJ*, 672, 214
Galliano, F., Madden, S. C., Jones, A. P., Wilson, C. D., & Bernard, J.-P. 2005, *A&A*, 434, 867
Galliano, F., Madden, S. C., Jones, A. P., *et al.*, 2003, *A&A*, 407, 159
Galliano, F., Madden, S. C., Tielens, A. G. G. M., Peeters, E., & Jones, A. P. 2008b, *ApJ*, 679, 310
Hunter, D. A., Gallagher, III, J. S., Rice, W. L., & Gillett, F. C. 1989, *ApJ*, 336, 152
Kennicutt, Jr., R. C. 1998, *ApJ*, 498, 541
Kunth, D. & Östlin, G. 2000, *A&A Rev.*, 10, 1
Madden, S. C., Galliano, F., Jones, A. P., & Sauvage, M. 2006, *A&A*, 446, 877
Meixner, M., Gordon, K. D., Indebetouw, R., *et al.*, 2006, *AJ*, 132, 2268
O'Halloran, B., Satyapal, S., & Dudik, R. P. 2006, *ApJ*, 641, 795
Reach, W. T., Rho, J., Jarrett, T. H., & Lagage, P.-O. 2002, *ApJ*, 564, 302
Rho, J., Kozasa, T., Reach, W. T., *et al.*, 2008, *ApJ*, 673, 271
Thuan, T. X., Sauvage, M., & Madden, S. 1999, *ApJ*, 516, 783
Wu, Y., Charmandaris, V., Hao, L., *et al.*, 2006, *ApJ*, 639, 157